Hindawi Publishing Corporation
Mathematical Problems in Engineering
Volume 2012, Article ID 937480, 15 pages
doi:10.1155/2012/937480

Research Article

Prediction of Inelastic Response Spectra Using Artificial Neural Networks

Edén Bojórquez,[1] Juan Bojórquez,[2] Sonia E. Ruiz,[2] and Alfredo Reyes-Salazar[1]

[1] *Facultad de Ingeniería, Universidad Autónoma de Sinaloa, Calzada de las Américas y Boulevard Universitarios S/N, Ciudad Universitaria, 80040 Culiacán Rosales, SI, Mexico*
[2] *Coordinación de Mecánica Aplicada, Instituto de Ingeniería, Universidad Nacional Autónoma de México, Ciudad Universitaria, 04510 Coyoacán, DF, Mexico*

Correspondence should be addressed to Edén Bojórquez, ebojorq@uas.uasnet.mx

Received 4 July 2012; Revised 20 August 2012; Accepted 21 August 2012

Academic Editor: Xu Zhang

Several studies have been oriented to develop methodologies for estimating inelastic response of structures; however, the estimation of inelastic seismic response spectra requires complex analyses, in such a way that traditional methods can hardly get an acceptable error. In this paper, an Artificial Neural Network (ANN) model is presented as an alternative to estimate inelastic response spectra for earthquake ground motion records. The moment magnitude (M_W), fault mechanism (F_M), Joyner-Boore distance (d_{JB}), shear-wave velocity (V_{s30}), fundamental period of the structure (T_1), and the maximum ductility (μ_u) were selected as inputs of the ANN model. Fifty earthquake ground motions taken from the NGA database and recorded at sites with different types of soils are used during the training phase of the Feedforward Multilayer Perceptron model. The Backpropagation algorithm was selected to train the network. The ANN results present an acceptable concordance with the real seismic response spectra preserving the spectral shape between the actual and the estimated spectra.

1. Introduction

The response spectrum is one of the most useful tools in earthquake engineering. In fact, earthquake-resistant design is based on the use of response spectra to estimate the seismic demand on structures. The response spectrum concept was used for the first time by Benioff [1], and subsequently by Housner [2] and Biot [3]. Nowadays, seismic design codes around the world use response spectra to establish the design forces. Hence, several studies have tried to establish methodologies to estimate elastic and inelastic response spectra; in particular, the estimation of inelastic seismic response spectra requires complex numerical

analysis, implying a great challenge in predicting the nonlinear structural response. This study proposes, as an alternative to estimate inelastic response spectra, the use of Artificial Neural Networks.

ANNs have been used widely around the world in earthquake engineering during the last years; its versatility to solve nonlinear and complex problems turn it into an alternative tool to search solutions for problems that require complex analysis. Alves [4] used neural networks for predicting seismic events, Lee and Han [5] used five models of ANN to generate artificial earthquakes and elastic seismic response spectra, and Kerh and Ting [6] trained a Backpropagation model to estimate the peak ground acceleration as a function of the distance to the epicenter, the hypocenter deepness, and the earthquake magnitude; with this study they designed the high speed lines of railways in Taiwan. Barrile et al. [7] through the use of a neuronal network model predicted the aftershocks related to large earthquakes, by the same time several studies have been developed to estimate the peak ground acceleration (García et al. [8], K. Günaydn and A. Günaydn [9], and Arjun and Kumar [10]). In the field of structural engineering, Papadrakakis and Lagaros [11] and Cheng and Li [12] applied ANN to structural reliability analysis. Moreover, Alcántara et al. [13] suggested the use of ANN to estimate elastic response spectra. In spite of the important contributions of the above mentioned studies, they were based on the prediction of peak ground acceleration or elastic response spectrum, and it is necessary to predict inelastic seismic response spectra.

Motivated by all the successful applications of ANN to solve elastic problems, in this study ANN is used as a tool to estimate inelastic seismic response spectra for earthquake ground motions recorded at stations located at different types of soils and originated by events of different source characteristics. In the next parts of the study, the definition of the seismic response spectrum is given and some basics concepts of Artificial Neural Networks are described.

2. Seismic Response Spectrum

The seismic response spectrum can be graphically displayed as an element that integrates the maximum response of a single-degree-of-freedom system with some level of damping ratio ξ and ductility μ when subjected to ground acceleration $\ddot{u}_g(t)$. The seismic response may be defined by different parameters (displacements, velocities, accelerations, etc.). In this study, pseudo-acceleration will be used to estimate the seismic response spectra, and consequently it will be the parameter of the output network, which is directly related with the resistance required by an earthquake-resistant structure. Moreover, the spectral shape in terms of the pseudo-acceleration spectrum is a very important parameter related with the ground motion potential of an earthquake (Bojórquez and Iervolino [14]).

The idealized force-displacement relation of a structure subjected to an increasing load is shown in Figure 1. In this figure, the elastic and the inelastic behaviors are illustrated. The main difference between the elastic and the inelastic behavior is the capacity to dissipate energy when the system presents inelastic behavior. In Figure 1, the inelastic system behavior is represented by the well-known elasto-plastic curve which is commonly used in several seismic design codes around the world.

For earthquake engineering purposes, it is desirable to estimate the peak displacement of an inelastic system u_m due to the action of the earthquake ground motion and to compare this displacement with the peak displacement caused by the same excitation acting in the corresponding linear system u_o. The elastic system is assumed to have the same stiffness as

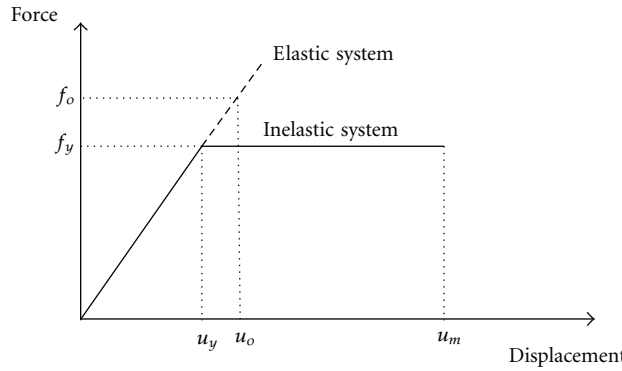

Figure 1: Force-displacement relationship of an inelastic system and its corresponding linear system.

that of the inelastic system during the initial loading. Both systems have the same mass and damping.

The normalized yield strength $\overline{f_y}$ of an inelastic system is defined as follows:

$$\overline{f_y} = \frac{f_y}{f_o} = \frac{u_y}{u_o}, \tag{2.1}$$

where $\overline{f_y}$ and u_y are the force and deformation at yielding.

If the normalized yield strength of a system is less than unity, the system will yield and deform into the inelastic range (e.g., $\overline{f_y} = 0.5$ implies that the yield strength of the system is one half of the minimum strength required for the system to remain elastic during the ground motion).

The procedure to obtain the seismic response spectrum for inelastic systems corresponding to specified levels of ductility is summarized as follows.

(1) Numerically define the earthquake ground motion $\ddot{u}_g(t)$.

(2) Select and fix the damping ratio ξ for which the spectrum is to be plotted.

(3) Select a value for the natural period of vibration of the system T_1.

(4) Estimate the response at each time instant $u(t)$ of the linear system with T_1 and ξ equal to the values previously selected. From $u(t)$ compute the peak deformation u_o and the peak force $f_o = k \cdot u_o$, where k is the stiffness of the system. Note that for the estimation of the elastic response spectra an iterative procedure is not required as in the case of the inelastic response spectra, where it is necessary to calculate the strength required to have a specific target ductility value, while in the elastic case the ductility is one.

(5) Determine the response $u(t)$ of an inelastic system with the same T_1 and ξ and yield force $\overline{f_y} = \overline{f_y}.f_o$, for a selected $\overline{f_y} < 1$. From $u(t)$ determine the peak deformation u_m and the associated ductility factor ($\mu_u = u_m/u_y$). Repeat the analysis for several values of $\overline{f_y}$ to develop data points ($\overline{f_y}, \mu_u$,) until the target ductility is obtained.

(6) Estimate the spectral ordinates corresponding to the value of $\overline{f_y}$ computed in step 5 associated to the target ductility. The pseudo-spectral acceleration is obtained as

Sa = $((2 \cdot \pi)/T_1)^2 \cdot u_m$, corresponding to the ordinate of one point on the spectrum with abscissa equal to T_1.

(7) Repeat steps 3 to 6 for a wide range of natural vibration periods.

For further information about seismic response spectra see Chopra [15].

The response spectrum for inelastic system developed according to this procedure can be used to establish the seismic design forces for ductile structures. The design forces of an inelastic system are smaller than the design forces of its corresponding elastic system, implying smaller sections of the structural members. In other words, elastic seismic designs are more expensive than inelastic seismic designs. The knowledge of the inelastic seismic response of structures is important in earthquake engineering due to the economical optimization of earthquake-resistant structures.

3. Artificial Neural Networks

The theory of Artificial Neural Networks arises from the need of solving complex problems, not only as a sequence of steps, but also as the evolution of computational systems inspired by the human brain and therefore endowed with certain "intelligence." An ANN is a mathematical or a computational model inspired by the structure and functional aspects of biological neural networks. The structure of a neural network is as follows: neurons are the main processing element, these are connected to other neurons via a signal weight (synapse), the entries are the dendrites, and the result is the axon (Figure 2). As in the case of neural networks, the ANN needs a process of learning to establish relationships between the variables that define a specific phenomenon. The processing power of an ANN is due to its distributed parallel structure, and the ability to learn from some examples, obtaining acceptable results from patterns never shown to it.

There are many topologies established by different authors to define the structure of the ANN; nevertheless, in this work the Feedforward Multilayer Perceptron (FMP) was selected (Shepherd, [16]). Figure 3 illustrates the architecture of the FMP. The architecture begins with an input layer which is connected to a hidden layer; this can be connected to another hidden layer or directly to the output layer. Because the information flow is always from the input layer to the output layer, the output of a layer is always the input of the next layer.

The training of the ANN used in this study was carried out using the "Backpropagation" algorithm proposed by Rumelhart and McClelland [17]. The procedure is as follows:

(1) A set of patterns consisting of pairs of inputs and outputs is applied to the network.

(2) The input data information is entered through the first layer. This information is propagated over the network according to a propagation rule: the entries are multiplied by the weights of the connection between layers, and the output is transformed by a nonlinear function and transferred to the next layer (there are several transfer functions, e.g., step, linear, mixed, Gaussian, hyperbolic tangent, secant hyperbolic, and sigmoid). Many investigations have used a sigmoid transfer function in the hidden layers and linear function in the output layer getting satisfactory results. For this reason herein the sigmoid function was selected as propagation rule. The same procedure is applied to the following layers until the output of the network is obtained.

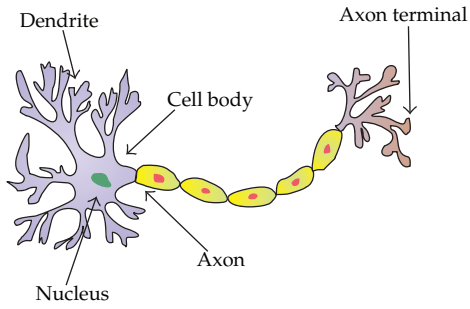

Figure 2: Schematic of biological neuron.

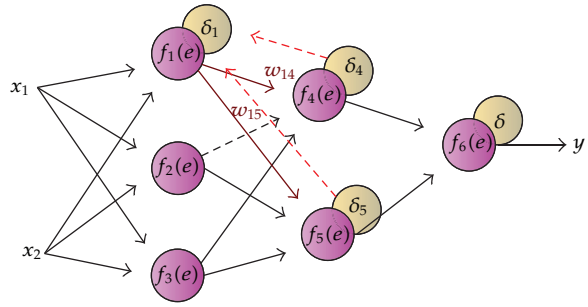

Figure 3: Feedforward Multilayer Perceptron.

(3) The results of the ANN model are compared with the target values of the spectral ordinates and the error is calculated.

(4) The error in the output layer is propagated backwards from the output layer through the hidden layers until the entrance is reached, so that all the neurons receive a certain percentage of error.

(5) Considering the received amount, each neuron makes an adjustment to its connection weights.

(6) The procedure is repeated with other input pairs until the error is less than a small tolerance, and the predicted inelastic response spectra tend to be as close as possible as the actual spectra.

The earthquake ground motion records selected for the analysis procedure are described in the following section.

4. Earthquake Ground Motion Records Characteristics

To observe the potential of ANN to predict inelastic response spectra, a total of fifty ground motion records obtained from the NGA database, corresponding to worldwide earthquakes, were used for the analyses. The records used for this study were selected from earthquakes with moment magnitudes (M_w) ranging from 5.9 to 7.7, and they have been taken from sites at Joyner and Boore distances (Joyner and Boore, [18]) between 18 and 194 kms, representing moderate and large earthquakes.

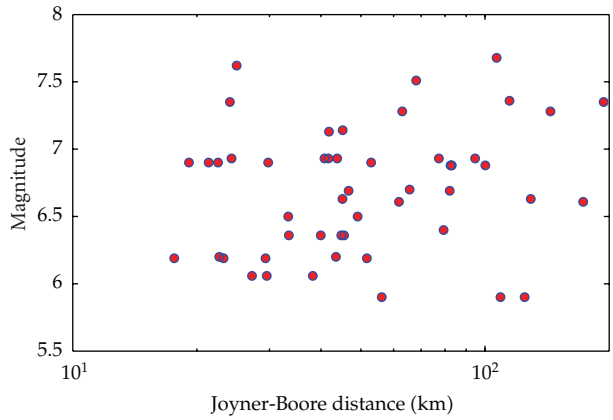

Figure 4: Moment magnitude and d_{JB} distance distribution for the selected 50 records taken from the NGA database.

The distribution of the records in terms of moment magnitude and d_{JB} distances is provided in Figure 4. In this figure, it can be observed that the records were obtained for different distances and from different events as moment magnitudes indicate; the wide range of the selected distances and magnitudes is very important for the training of the Artificial Neural Networks.

Tables 1, 2, 3, 4, and 5 summarize the main characteristics of the seismic records used in this study (corresponding to all types of soil zones in accordance with the shear-wave velocity). Soil type A corresponds to rock and soil type E to soft soil. In the tables, the first column refers to the record number, the second column corresponds to the moment magnitude of the event, the fourth column refers to the Joyner and Boore distance, and the last column is the shear wave velocity above site depth of 30 m. In the next subsections, the definition of the failure type (column 3) and the soil type are given.

4.1. Failure Mechanisms

The selected ground motion records were generated by four different failure mechanisms: Longitudinal (0), Normal (1), Reverse (2), and Oblique (3). It is observed that for the selection of the record accelerations there were considered an average of 12 records for each type of failure, so that ANN could generalize the estimation of spectra coming from motions corresponding to different type of failure mechanism. The use of different record features is very helpful to reduce the error in the estimation of inelastic response spectra. Figure 5 shows the number of events corresponding to each type of failure mechanism.

4.2. Types of Soil

As stated earlier five soil types are used in this study. They are expressed as a function of shear-wave velocity. Table 6 illustrates the soil type as a function of shear-wave velocity, as classified by NEHRP. Note that soil type A represents a very hard soil, while soil types E corresponds to a soft soil. Ten records were selected for each soil type.

Table 1: Ground motion records for soil type A.

Record	Moment magnitude	Failure type	d_{JB} distance	V_{s30} (m/s)
1	6.61	2	61.79	1735
2	6.9	1	52.93	1562.2
3	6.36	2	40.01	1676.1
4	6.88	1	100.22	1559.6
5	6.19	0	23.23	1862.2
6	6.06	3	38.22	1684.9
7	6.93	3	41.68	1815.3
8	7.28	0	144.13	1946
9	6.69	2	46.65	1821.7
10	7.68	0	106.71	1659.6

Table 2: Ground motion records for soil type B.

Record	Moment magnitude	Failure type	d_{JB} distance	V_{s30} (m/s)
1	6.63	0	129.11	1328.6
2	6.5	2	49.13	1274.4
3	6.88	1	82.6	1274.4
4	6.06	3	27.21	1112.4
5	7.14	0	45.16	1413
6	7.13	0	41.82	814.3
7	6.36	2	45.49	1315
8	6.36	2	33.42	1015.6
9	6.88	1	83	1274.4
10	6.06	3	29.56	1015.6

Table 3: Ground motion records for soil type C.

Record	Moment magnitude	Failure type	d_{JB} distance	V_{s30} (m/s)
1	6.61	2	173.16	388.5
2	7.35	2	24.07	368.2
3	6.9	1	29.79	532.7
4	6.2	1	22.68	530
5	6.36	2	44.82	438.5
6	6.7	0	65.67	548.6
7	6.19	0	29.35	738.5
8	6.93	3	40.85	449.6
9	7.28	0	62.98	645.4
10	6.4	1	79.33	598.6

From Figures 4 and 5, and Tables 1, 2, 3, 4, and 5, it can clearly be seen that the selected ground motion records cover a wide range of earthquake sources and site characteristics.

5. Artificial Neural Network Model

The aim of this part of the study is to implement Artificial Neural Networks to estimate inelastic response spectra using the Multilayer Perceptron (Backpropagation). To achieve this

Table 4: Ground motion records for soil type D.

Record	Moment magnitude	Failure type	d_{JB} distance	V_{s30} (m/s)
1	7.36	2	114.62	253.2
2	6.19	0	17.64	327.1
3	6.63	0	45.12	180.8
4	6.5	2	33.32	319.6
5	7.35	2	193.91	219.6
6	6.2	1	43.5	359.6
7	6.93	3	24.27	191.8
8	6.69	2	82.03	296.6
9	7.62	3	24.98	188.1
10	6.9	1	22.54	320

Table 5: Ground motion records for soil type E.

Record	Moment magnitude	Failure type	d_{JB} distance	V_{s30} (m/s)
1	6.9	0	21.35	151.2
2	7.51	0	68.09	175
3	6.9	0	19.14	164
4	6.93	3	77.32	155.1
5	6.93	3	94.56	169.7
6	6.93	3	43.77	116.4
7	6.19	0	51.68	146
8	5.9	2	56.17	176
9	5.9	2	109.02	173
10	5.9	2	124.87	156

Table 6: Soil types under consideration.

Soil type	Soil condition	V_{s30} (m/s)
A	Hard Rock	>1500
B	Rock	760–1500
C	Soft Rock	360–760
D	Deep Rock	180–360
E	Clay	<180

objective, in the first place, appropriate parameters must be selected for the training phase, and in the second places, it is necessary to find the optimal network architecture. The most important limitation of ANN is that its efficiency depends on the training algorithm and network architecture. Unfortunately, there are no rules for determining both characteristics of the network. Only by using the trial and error procedure it is possible to find the optimal network. In order to obtain satisfactory results with the Backpropagation algorithm it is necessary that the values of the training vector represent the entire domain of the output. The proper selection of training parameters is an important issue for training Artificial Neural Networks.

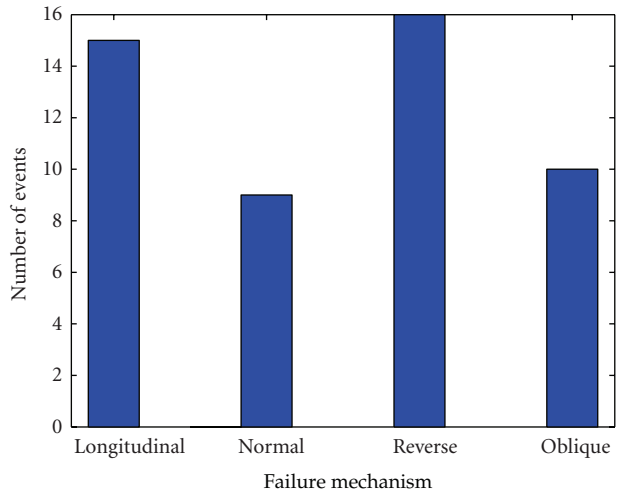

Figure 5: Distribution of selected failure mechanisms.

5.1. Estimation of Input and Output Parameters

An appropriate selection of the parameters that represent an ANN is required for the correct working of the network. The parameters required to estimate the seismic response spectra in terms of pseudo-acceleration are moment magnitude, mechanism of failure, Joyner-Boore distance, shear-waves velocity, fundamental period of vibration of the system and maximum ductility. According to the above, inputs to the network are defined here by the values of M_w, F_M, d_{JB}, V_{s30}, T_1, and μ_u. The output node is represented by the pseudo-acceleration at first mode of vibration $\mathrm{Sa}(T_1)$. The values of the input parameters are shown in Tables 1 and 6, and the input range values are presented in Table 7. Note that the input parameters are usually selected to propose ground motion attenuation prediction equations, and the chosen ductility levels are commonly used for the seismic design of buildings.

5.2. Architectures Used for the ANN Model

A large number of architectures were tested in order to obtain the best ANN model. The format for the architecture arrangements shown in Table 8 is described by $I \times H_1 \times H_2 \times \cdots H_i \times O$, where I represents the number of neurons in the input layer; H_i represents the number of neurons in the ith hidden layer; O represents the number of neurons in the output layer. Table 8 shows some of the models that were used. In this table we can see that models with more than one hidden layer have a lower total error in the training phase compared with one hidden layer models. Nevertheless, these models in the testing phase generated a much higher total error than models with one hidden layer. This is because the model is overtrained and the network estimates the spectra in the training phase with very good accuracy; however, the same is not valid for the testing phase, which implies that the network could not be generalized.

It turned out that the optimal architecture for this problem is a multilayer neural network with feedforward. The selection of the optimal architecture of an ANN is not an easy task as it is necessary to test a large number of architectures to achieve the best one. In

Table 7: Range of input parameters for the neural network.

Input	Range
M_w	5.9–7.7
F_M	0–3
d_{JB}	18–194 km
V_{s30}	116–1946 m/s
T_1	0–3 sec
μ_u	1–6

Table 8: Proposed architectures.

Architecture	Iterations	Total error
6 × 50 × 1	73	0.13
6 × 75 × 1	56	0.12
6 × 100 × 1	165	0.082
6 × 125 × 1	186	0.093
6 × 30 × 60 × 1	338	0.095
6 × 50 × 60 × 1	498	0.087
6 × 90 × 60 × 1	657	0.084
6 × 100 × 50 × 1	865	0.077
6 × 30 × 30 × 30 × 1	1823	0.069
6 × 50 × 50 × 50 × 1	1435	0.073
6 × 100 × 100 × 100 × 1	2181	0.057

this paper, under the authors' judgment, it was assumed that the optimal model architecture consists of an input layer, one hidden layer, and one output layer, with the topology $6 \times 100 \times 1$ which means that 6, 100, and 1 neurons were used in the input, hidden and output layers, respectively (see Table 8).

6. ANN Model, Training, and Testing Phases

As it was described before, the Backpropagation algorithm was selected for the training phase. The transfer functions used in the network layers were sigmoid for the hidden layer and linear function for the output layer. During training it was found that the ANN had trouble in estimating the inelastic response spectra, so it was necessary to test a large number of architectures. To train and test the ANN models, a computer program was developed that includes routines for MATLAB Neural Network Tool Box (Demuth et al. [19]). The selection of training parameters was such that the ANN had a predictive capability for events not used during training. Figure 6 shows the regression results in the networks training, which compares the value estimated by the network and the actual value. While Figure 6(a) shows the 6 × 100 × 1 Model, Figure 6(b) illustrates the 6 × 100 × 100 × 100 × 1 Architecture. The regression line indicates the precision of the ANN in the estimation of the real value of the spectral acceleration; the error in the training phase is represented by the slope of the line (an ideal ANN model should have a 1 : 1 slope). It is observed that for both cases the slope of the regression line is almost 1, which implies that the model predicts with good accuracy the spectral acceleration. Although for Case b the error estimated in the training is slightly lower than the error for Case a, in the test phase the error produced by the network corresponding

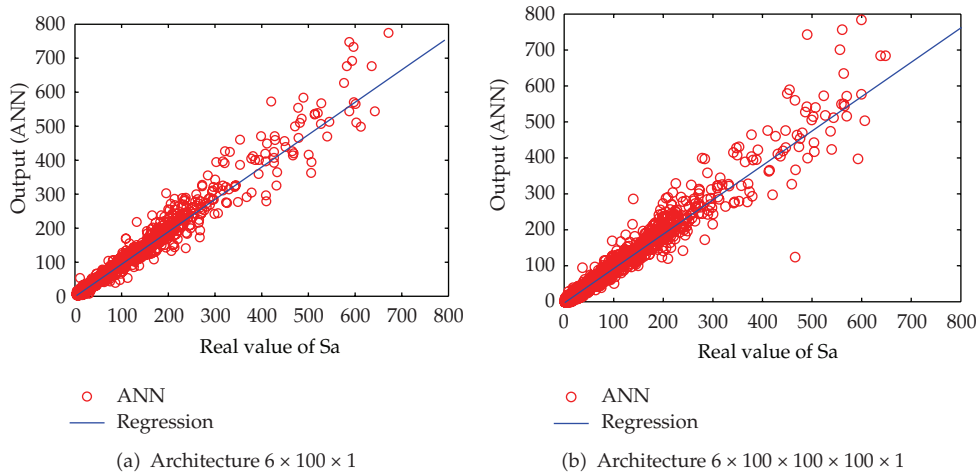

(a) Architecture 6 × 100 × 1 (b) Architecture 6 × 100 × 100 × 100 × 1

Figure 6: Comparison of the regression results of the ANN corresponding to the training phase.

to case b was much larger than that corresponding to case a. This is due to the "overlearning" problem, which has been observed in all the networks with two or more hidden layers.

6.1. Training Results

Figures 7(a)–7(d) compare the inelastic seismic response spectra for different ductility levels and soil types obtained during the training phase (dashed line) with the actual spectra computed with the real records (solid line). The results of the training stage show an acceptable relation between the predicted and the real spectra. The maximum error between the actual response spectra and that obtained with ANN was 12%. It is observed that the spectral shape presents a clear definition throughout the range of periods. This is very important because the spectral shape of the pseudo-acceleration spectrum is an indicator of the ground motion potential of an earthquake (Bojórquez and Iervolino [14], Bojórquez et al. [20]); moreover, ground motion intensity measures based on spectral shape are very useful to estimate the seismic fragility of buildings in terms of peak and energy demands (Bojórquez et al. [21], Bojórquez et al. [22]). The control of seismic energy demands is very important on structures subjected to long duration ground motion records (Teran-Gilmore and Jirsa [23], Bojorquez et al. [24]). Note that the shape of the spectra shown in Figures 7(a)–7(d) is very similar for different nonlinear levels and types of soil, which suggests that the training of the ANN model was satisfactory.

6.2. Test Results

After the training gave adequate results, in the test phase some random records were chosen from the NGA database in order to test the network (these records were never shown to the ANN model). The test phase results are shown in Figures 8(a)–8(d). Note that in the testing stage the ANN results are shown to be as good as those obtained during the training stage; in fact, the results shown in Figures 8(a)–8(d) indicate a very good relationship between the predicted spectra via ANN and the real spectra; this is valid for different types of soils and ductility levels. It is observed that the ANN model keeps its spectral shape in all the cases.

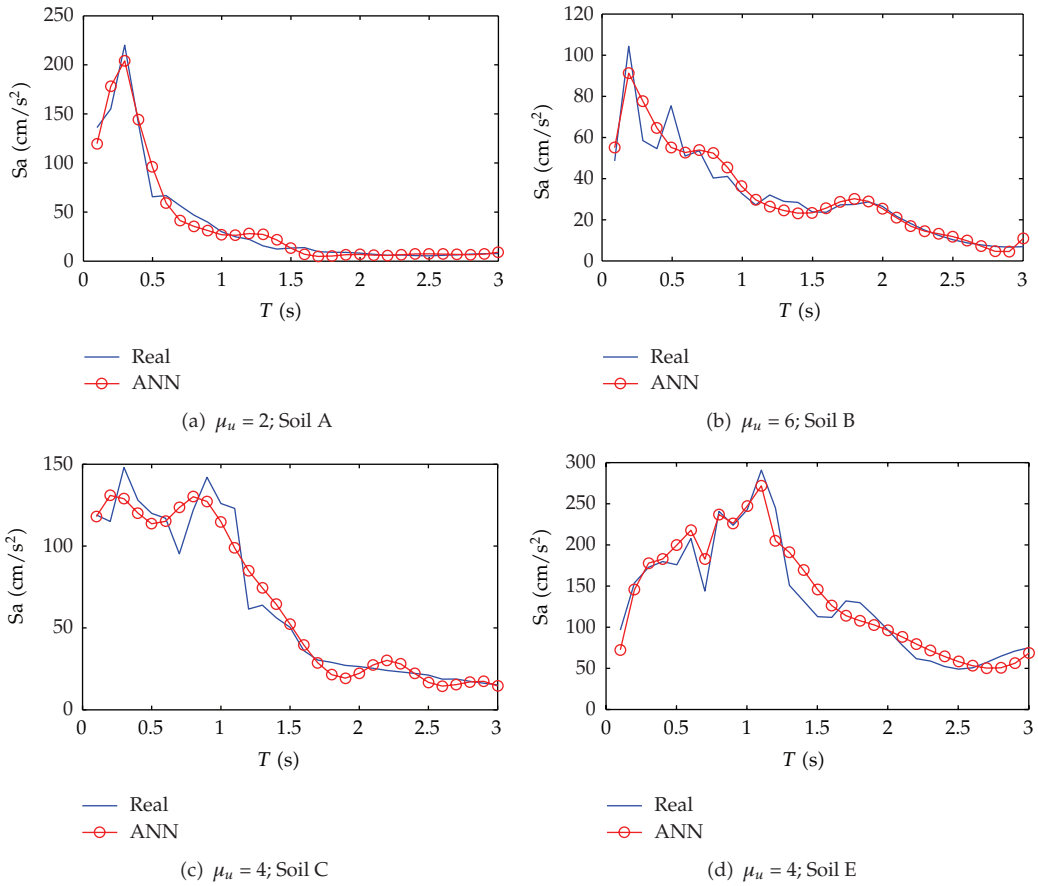

Figure 7: Comparison of earthquake response spectra obtained during the training phase (ANN versus real).

Note that the results presented in Figures 8(a), 8(b), 8(c) and 8(d) correspond to zones A, B, C, and E, respectively, for one random record. Similar results were found for other analyzed records.

The results of the ANN model to estimate inelastic response spectrum corresponding to different accelerations records are acceptable. It is observed that the error in the estimation increases as ductility gets larger. When estimating response spectra for different soil types, the network presents more difficulties in estimating spectra for soil type E than for soil type A; hence the estimation, of the spectra for soft soils generates a higher error than for intermediate or stiff soils. This is because there is more uncertainty when soft soil records are considered to estimate nonlinear structural response. The most important observation is that the ANN model retains all the characteristics of the spectral shape of the earthquake response spectra, which is a crucial aspect related to the ground motion potential of an earthquake.

7. Conclusions

An Artificial Neural Network model to estimate inelastic seismic response spectra for different types of soils and seismicity zones is proposed. The moment magnitude of the event,

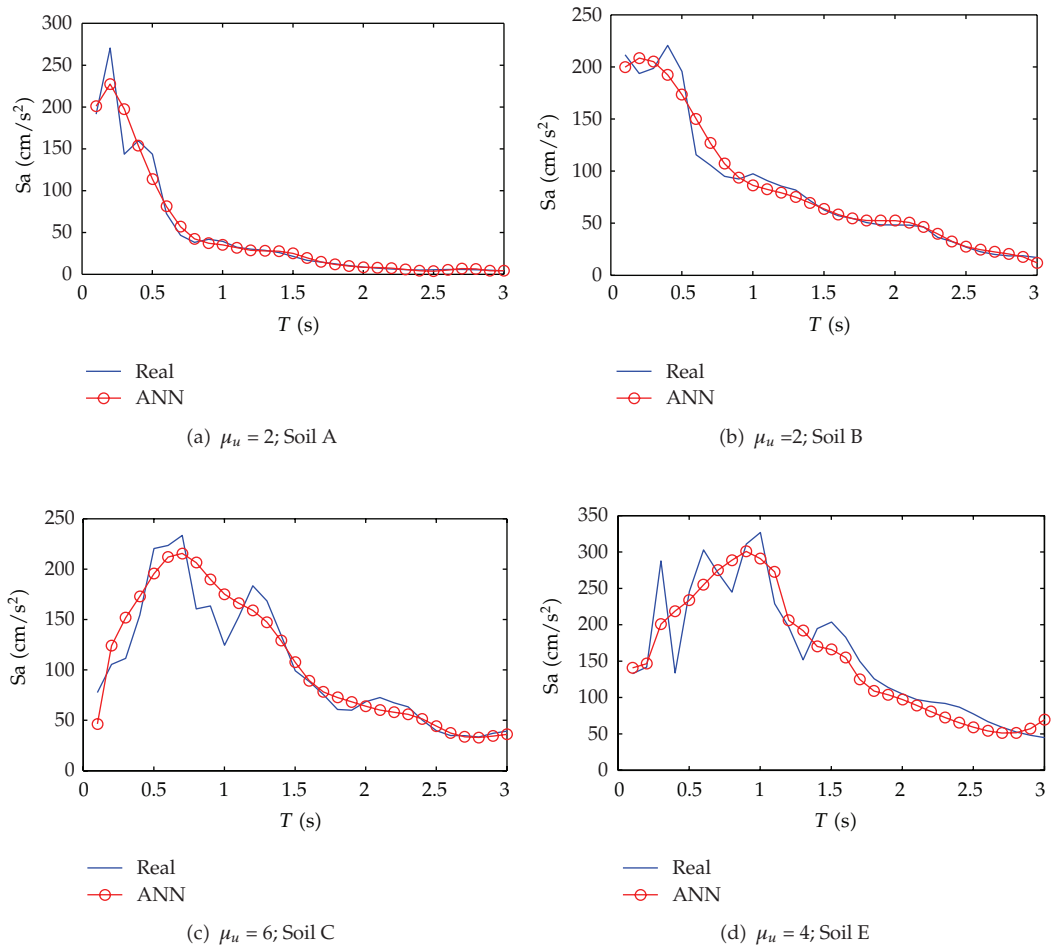

Figure 8: Comparison of earthquake response spectra obtained during the testing phase (ANN versus real).

mechanism of failure, Joyner and Boore distance, shear-wave velocity, fundamental period of the structure, and ductility were selected as the inputs for the ANN model. The output was represented by the spectral pseudo-acceleration response. It is important to say that the input parameters selected are usually used to propose ground motion attenuation prediction equations.

It is concluded that the ANN model proposed to estimate inelastic seismic response spectra gives an acceptable concordance when compared to that of the real spectra. The main conclusion is that the ANN represents a good accuracy for estimating the elastic response spectra, since it gives the lowest error. In the case of the inelastic spectra, the error increases as the ductility increases; however, the error in the estimation of inelastic spectra using the ANN model is acceptable; more importantly, it preserves the spectral shape of the real response spectra.

It is suggested that for successful operation of the ANN model, it is essential to select properly the architecture, method and learning algorithms as well as the main parameters that represent the specific problem under consideration.

Acknowledgments

The support given by El Consejo Nacional de Ciencia y Tecnología to the first author under grant CB-2011-01-167419 and the scholarship to the second author is appreciated. Financial support also was received from the Universidad Autónoma de Sinaloa under grant PROFAPI 2011/029, and from the Universidad Nacional Autónoma de México under project PAPIIT-IN109011-3.

References

[1] H. Benioff, "The physical evaluation on seismic destructiveness," *Bulletin of the Seismological Society of America*, vol. 24, pp. 398–403, 1934.

[2] G. Housner, *An investigation of the effects of earthquakes on buildings [Ph.D. thesis]*, California Institute of Technology, Pasadena, Calif, USA, 1941.

[3] M. A. Biot, "A mechanical analyzer for the prediction of earthquake stresses," *Bulletin of the Seismological Society of America*, vol. 31, no. 2, pp. 151–171, 1941.

[4] E. I. Alves, "Earthquake forecasting using neural networks: results and future work," *Nonlinear Dynamics*, vol. 44, no. 1–4, pp. 341–349, 2006.

[5] S. C. Lee and S. W. Han, "Neural-network-based models for generating artificial earthquakes and response spectra," *Computers and Structures*, vol. 80, no. 20-21, pp. 1627–1638, 2002.

[6] T. Kerh and S. B. Ting, "Neural network estimation of ground peak acceleration at stations along Taiwan high-speed rail system," *Engineering Applications of Artificial Intelligence*, vol. 18, no. 7, pp. 857–866, 2005.

[7] V. Barrile, V. Cacciola, S. D'Amico, A. Greco, F. C. Morabito, and F. Parrillo, "Radial basis function neural networks to foresee aftershocks in seismic sequences related to large earthquakes," in *Proceedings of the 13th International Conference on Neural Information Processing*, vol. 4233, pp. 909–916, 2006.

[8] S. R. García, M. P. Romo, and J. M. Mayoral, "Estimation of peak ground accelerations for Mexican subduction zone earthquakes using neural networks," *Geofisica Internacional*, vol. 46, no. 1, pp. 51–63, 2007.

[9] K. Günaydn and A. Günaydn, "Peak ground acceleration prediction by artificial neural networks for northwestern Turkey," *Mathematical Problems in Engineering*, vol. 2008, Article ID 919420, 20 pages, 2008.

[10] C. R. Arjun and A. Kumar, "Artificial neural network-based estimation of peak ground acceleration," *Journal of Earthquake Technology*, vol. 46, pp. 19–28, 2009.

[11] M. Papadrakakis and N. D. Lagaros, "Reliability-based structural optimization using neural networks and Monte Carlo simulation," *Computer Methods in Applied Mechanics and Engineering*, vol. 191, no. 32, pp. 3491–3507, 2002.

[12] J. Cheng and Q. S. Li, "Reliability analysis of structures using artificial neural network based genetic algorithms," *Computer Methods in Applied Mechanics and Engineering*, vol. 197, no. 45–48, pp. 3742–3750, 2008.

[13] L. Alcántara, E. Ovando, and M. A. Macías, "Estimación de espectros de respuesta en la ciudad de puebla utilizando redes neuronales artificiales," in *XVI Congreso Nacional de Ingeniería Sísmica*, Puebla, México, 2009.

[14] E. Bojórquez and I. Iervolino, "Spectral shape proxies and nonlinear structural response," *Soil Dynamics and Earthquake Engineering*, vol. 31, no. 7, pp. 996–1008, 2011.

[15] A. K. Chopra, *Dynamics of Structures, Theory and Applications to Earthquake Engineering*, Prentice-Hall, Upper Saddle River, NJ, USA, 2nd edition, 2001.

[16] G. M. Shepherd, *The Synaptic Organization of the Brain*, Oxford University Press, 4th edition, 1997.

[17] D. E. Rumelhart and J. L. McClelland, *Parallel Distributed Processing. Foundations*, MIT Press, 1986.

[18] W. B. Joyner and D. M. Boore, "Methods for regression analysis of strong-motion data," *Bulletin of Seismological Society of America*, vol. 83, no. 2, pp. 469–487, 1993.

[19] H. Demuth, M. Beale, and M. Hagan, *Neural Network Toolbox: For Use With Matlab*, Mathworks, Natick, Mass, USA, 2009.

[20] E. Bojórquez, I. Iervolino, and G. Manfredi, "Evaluating a new proxy for spectral shape to be used as an intensity measure," in *Proceedings of the Seismic Engineering Conference Commemorating the 1908 Messina and Reggio Calabria Earthquake*, vol. 1020, pp. 1599–1606, 2008.

[21] E. Bojórquez, A. Terán-Gilmore, S. E. Ruiz, and A. Reyes-Salazar, "Evaluation of structural reliability of steel frames: inter-story drifts versus plastic hysteretic energy," *Earthquake Spectra*, vol. 27, no. 3, pp. 661–682, 2011.

[22] E. Bojórquez, I. Iervolino, A. Reyes-Salazar, and S. E. Ruiz, "Comparing vector-valued intensity measures for fragility analysis of steel frames in the case of narrow-band ground motions," *Engineering Structures*, vol. 45, pp. 472–480, 2012.

[23] A. Teran-Gilmore and J. O. Jirsa, "Energy demands for seismic design against low-cycle fatigue," *Earthquake Engineering and Structural Dynamics*, vol. 36, no. 3, pp. 383–404, 2007.

[24] E. Bojorquez, S. E. Ruiz, and A. Teran-Gilmore, "Reliability-based evaluation of steel structures using energy concepts," *Engineering Structures*, vol. 30, no. 6, pp. 1745–1759, 2008.